Effect of Parametric Variation of Center Frequency and Bandwidth of Morlet Wavelet Transform on Time-frequency Analysis of Event-related Potentials

Guanghui Zhang[1,2], Lili Tian[3], Huaming Chen[1], Peng Li[4], Tapani Ristaniemi[2], Huili Wang[3], Hong Li[4], Hongjun Chen[3], Fengyu Cong[1,2]

Abstract. Time-frequency (TF) analysis of event-related potentials (ERPs) using Complex Morlet Wavelet Transform has been widely applied in cognitive neuroscience research. It has been widely suggested that the center frequency (*fc*) and bandwidth (σ) should be considered in defining the mother wavelet. However, the issue how parametric variation of *fc* and σ of Morlet wavelet transform exerts influence on ERPs time-frequency results has not been extensively discussed in previous research. The current study, through adopting the method of Complex Morlet Continuous Wavelet Transform (CMCWT), aims to investigate whether time-frequency results vary with different parametric settings of *fc* and σ. Besides, the nonnegative canonical polyadic decomposition (NCPD) is used to further confirm the differences manifested in time-frequency results. Results showed that different parametric settings may result in divergent time-frequency results, including the corresponding time-frequency representation (TFR) and topographical distribution. Furthermore, no similar components of interest were obtained from different TFR results by NCPD. The current research, through highlighting the importance of parametric setting in time-frequency analysis of ERP data, suggests that different parameters should be attempted in order to get optimal time-frequency results.

Keywords: Complex Morlet Wavelet Transform, event-related potentials, center frequency, bandwidth, time-frequency representation.

Guanghui Zhang, Lili Tian, Huaming Chen, Peng Li, Tapani Ristaniemi, Huili Wang, Hong Li, Hongjun Chen (✉), Fengyu Cong(✉)

1.Department of Biomedical Engineering, Faculty of Electronic Information and Electrical Engineering, Dalian University of Technology, 116024, Dalian, China.
E-mail: cong@dlut.edu.cn

2. Department of Mathematical Information Technology, University of Jyväskylä, 40014, Jyväskylä, Finland

3. School of Foreign Languages, Dalian University of Technology, 116024, Dalian, China
E-mail: chenhj@dlut.edu.cn

4. College of Psychology and Sociology, Shenzhen University, 518060, Shenzhen, China

1 Introduction

Electroencephalogram (EEG) has been extensively applied in cognitive neuroscience research. EEG, according to different experimental paradigms and external stimuli, can be divided into three categories: spontaneous EEG [1], event-related potentials (ERP) [2], and ongoing EEG [3]. The main methods employed in ERP data processing are as the following: 1) Time-domain analysis, 2) Frequency-domain analysis and 3) Time-frequency analysis [4-8]. As ERP signals are non-stationary and time-varying, neither the time-domain nor the frequency-domain analysis can be used to effectively reveal the time-frequency information of ERP data. Time-frequency analysis, by focusing on the time-varying features of ERP components, is conducted to transform a one-dimensional time signal into a two-dimensional time-frequency density function, which aims to reveal the number of frequency components and how each component varies over time.

In 1996, Tallon-Baudry *et al*. introduced the Morlet wavelet for time-frequency analysis of ERP data [9]. Since then, the Morlet wavelet has been widely applied by researchers in conducting time-frequency analysis, with its citations over 1100 times (From the Google scholar). However, a synthesis of previous research showed that in most cases the value of K is fixed ($\mathrm{e.g.}, K = 7$) [9-12], therefore leaving the issue whether parametric variation of fc and σ has an impact on time-frequency results unresolved. This study is devoted to investigation of the issue.

2 Method

2.1 Data Description

The data was collected to investigate whether a short delay in presenting an outcome affects brain activity. For the detailed information of experimental procedure, readers can refer to Wang *et al.* research [13]. Twenty-two undergraduates and graduate students participated in the experiment as volunteers. All the participants, aged from 18 to 24, were right-handed with normal or corrected-to-normal vision and no one was reported to have neurological or psychological disorders. EEG was recorded using a 64-channel system (Brian Products GmbH, Gilching, Germany) with reference on the left mastoid. The vertical and horizontal electrooculogram (EOG) was recorded from electrodes placed above and below the right eye and on the outer canthi of the left and right eyes respectively. Electrode impedance was maintained below 10k Ohm. The EEG and EOG were sampled continuously at 500Hz with 0.01-100Hz bandpass filtering.

2.2 Complex Morlet Wavelet Transform

The CMCWT method, based on the Complex Morlet Wavelets, was adopted for time-frequency analysis in the present study.

If *x(t)* is a discrete sequence of length *T*, the definition of the Continuous Wavelet Transform (CWT) can be expressed as follows:

$$X(a,b) = \frac{1}{\sqrt{|a|}} \sum_{t=0}^{T-1} x(t) \Phi \left(\frac{t-b}{a} \right). \quad (1)$$

In the above formula, *x(t)* represents the signal to be transformed; *a* refers to the scaling and *b* the time location or shifting parameters; $\Phi(t)$ stands for the mother wavelet. In this study, the Complex Morlet Wavelets is defined as the mother wavelet [9-12]:

$$\Phi(t, fc) = \frac{1}{\sqrt{\pi \sigma^2}} e^{i2\pi t f_c} e^{\frac{-t^2}{2\sigma^2}}. \quad (2)$$

According to the above formula, a Gaussian shape respectively in the time and frequency domain around its f_c can be obtained.
A wavelet family is characterized by a constant ratio:

$$K = {f_c}/{\sigma_f} = 2\pi\sigma f_c . \quad (3)$$

In this formula, $\sigma_f = {1}/{2\pi\sigma}$, K should be greater than 5 [9].
Taken together, this method (CMCWT) can be described as below:

$$\mathrm{CMCWT}(t,f) = |\Phi(t,f) * x(t)|^2. \quad (4)$$

In the above formula, '*' refers to convolution.

2.3 Nonnegative Canonical Polyadic Decomposition

Nonnegative Canonical Polyadic Decomposition (NCPD) has been widely applied to study time-frequency representation (TFR) of EEG [14, 15]. For example, given a third-order tensor including the modes of time, frequency and space, $\underline{\mathrm{X}} \in \mathcal{R}^{\mathrm{I}_1 \times \mathrm{I}_2 \times \mathrm{I}_3}$, the NCPD can be defined:

$$\underline{\mathrm{X}} = \sum_{r=1}^{R} t_r \circ f_r \circ s_r + \underline{E} = \sum_{r=1}^{R} \underline{X}_r + E = \widehat{\underline{\mathrm{X}}} + \underline{E} \approx \widehat{\underline{\mathrm{X}}} . \quad (5)$$

In this formula, the symbol '$\circ$' denotes the outer product of vectors. The t_r, f_r, and s_r correspond to the temporal component $\sharp\, r$, the spectral component $\sharp\, r$, and the spatial component $\sharp\, r$, and the three components reveal the properties of the multi-domain properties of an ERP in the time, frequency and space domains [14].

For the same multi-channel EEG data, different parameters of CMCWT may produce different TFR (indeed, third-order tensors in this study) in terms of visual inspection. Then, the application of NCPD on those tensors can assist to investigate whether the similar components of interest can be extracted from different tensors resulting different TFR parameters of the same EEG data. For the detailed

information of the number of extracted components for each mode, and the criteria of selecting multi-domain features, readers can refer to Cong *et al.* research [15].

3 Data Processing and Analysis

The ERP data were pre-processed in MATLAB and EEGLAB [16], including the following steps: a 50Hz notch filter to remove line noise, a low-pass filtering of 100Hz, segmentation of the filtered continuous EEG into single trials (each trial was extracted offline from 200ms pre-stimulus onset to 1000ms post-stimulus onset), baseline correction, artifact rejection and averaging.

In CMCWT analysis, the frequency range was set from 1 to 30Hz, respectively in 0.1 Hz step (*fc* = 9,10, respectively), in 0.2Hz step (*fc* = 5,6,7,8,9,10, respectively), in 0.3Hz step (*fc* = 3,4,5,6,7,8,9,10, respectively), in 0.4Hz step (*fc* = 3,4,5,6,7, 8,9,10, respectively), in 0.5Hz step (*fc* = 2,3,4,5,6,7,8,9,10, respectively), in 0.6Hz step (*fc* = 2,3, 4,5,6,7,8,9,10, respectively), in 0.7Hz (*fc* = 2,3,4,5,6,7,8,910, respectively), in 0.8Hz step (*fc* = 2,3,4,5,6,7,8,9,10, respectively), in 0.9Hz step (*fc* = 1,2, 3,4,5,6,7,8, 9,10, respectively) and in 1Hz step (*fc* = 1,2,3,4,5,6,7,8,9,10, respectively). All the above parametric settings met the requirement of constant ratio (greater than 5).

To further investigate whether parametric variation of *fc* and σ has an impact on time-frequency results, four steps are carried out in the following sequence:

(1) Select a typical topographical distribution of TFR results as the template. When $\sigma_0 = 1$, the value of *fc* can be respectively set as 1,2,3,4,5,6,7,8,9 and 10. The topographical distribution of $fc_4 = 4$ is finally chosen as the template $\mathrm{T}_{\mathrm{template}}(\sigma_0, fc_4)$ in terms of the prior knowledge of the ERP of interest.

(2) Define a fc_n, calculate the Correlation Coefficients (CCs) between the template ($\mathrm{Y}_{\mathrm{template}}$) and each spatial component $s_{\mathrm{r}}(\sigma_0, fc_n)$ obtained by NCPD (R components were extracted in each mode), which can be described as:

$$\mathrm{Y}(\sigma_0, fc_n, \mathrm{r}) = \rho\big(s_r(\sigma_0, fc_n), T_{template}(\sigma_0, fc_4)\big). \quad (6)$$

In the above formula, $\mathrm{r} = 1, 2, \cdots, 21, \mathrm{n} = 1, 2, \cdots, 10$. Subsequently, the maximal CC is chosen as:

$$\mathrm{q}(\sigma_0, fc_n) = \max\big(Y(\sigma_0, fc_n, 1), Y(\sigma_0, fc_n, 2), \cdots, Y(\sigma_0, fc_n, R)\big). \quad (7)$$

Then, the corresponding r^{th} components with the maximum CC were obtained.

(3) Based on the obtained components of each dimension and their corresponding TFR results, we need to judge whether the TFR results of different parameters are similar or not. The TFR results are different when the *fc* is respectively set as 1 and 9. Besides, the corresponding 16^{th} components of $fc_1 = 1$ and 1^{th} components of $fc_9 = 9$ are similar in the spacial dimension, but not the temporal and spectral dimension (as shown in the first and third row of Figure 4).

(4) With the same procedure mentioned above, we can analyze the results of other σ and *fc* parameters to explore potential differences in the time-frequency results.

4 Results

Results showed that parametric variations of σ and *fc* lead to different time-frequency representation and topographical distribution. The data results shown in Figure 1, Figure 2, Figure 3, Figure 4 and Figure 5 are all from one subject in one condition (short-gain condition), and the data used for statistical analysis (Figure 6) are from 22 subjects in four conditions (waiting time (short, long)$\times$feedback valence (loss, gain)). Due to the space limitation, only the results of $\sigma = 1$, *fc* = 1,2,3,4,5,6,7,8,9,10 are presented here.

Figure 1 shows the waveform at Cz electrode in the left panel and the waveform of all channels in the right. From the waveform, certain ERP components can be recognized. As shown in Figure 2, the comparison of the TFR results of *fc* = 1,2,3,4,5 with other parameters (*fc* = 6,7,8,9,10) shows differences in the time frequency resolution. In Figure 3, the topographical distributions are obtained by averaging the area of each rectangle. Within the time window of 100-400ms and frequency range of 7-10Hz, it can be observed that the topographical distributions are highly similar among each other when *fc* = 1,2,3,4,5,6,7,8.

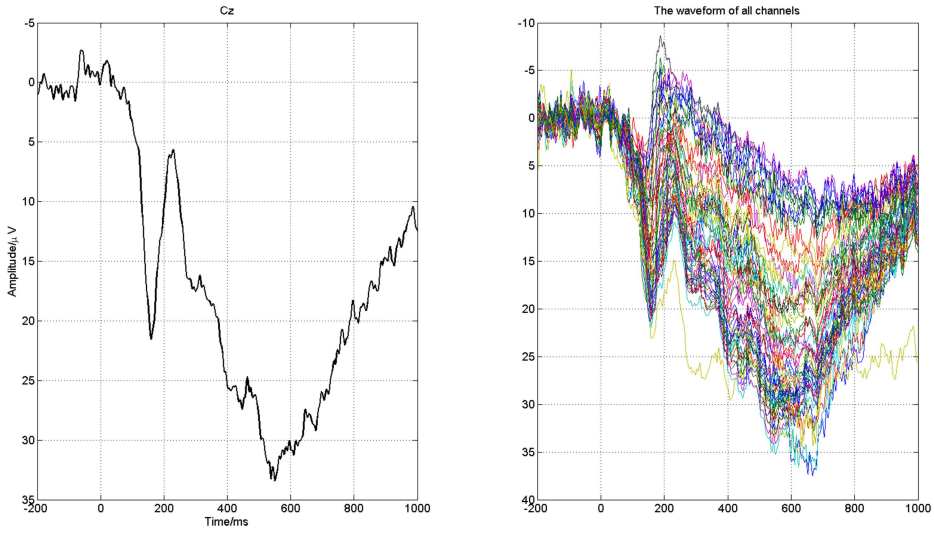

Figure 1 Waveforms at Cz and all channels

As shown in Figure 4, the topographical distribution of *fc* = 4 is selected as the template. The correlation coefficient values between the template and the three components of spatial dimension (the fourth column) are respectively 0.8495, 0.8947 and 0.8915. A comparison of the waveform, spectrum, TFR and topographical distribution in first row (or the second row) with those of the third row shows commonalities only in the topographical distribution, but not waveform, spectrum and TFR. As shown in Figure 5, the time window is from 100 to 400ms and the frequency from 7 to 10Hz. In Figure 5(a), different lines represent different σ; in Figure 5(b),

different lines represent different *fc*. The topographical distribution of $\sigma = 1, fc = 4$ is chosen as the template. Then, correlation analyses are conducted between the topographical distributions of each parameter and the template. When σ (or *fc*) is fixed, the correlation coefficient shows a decreasing tendency with the increasement of *fc* (or σ).

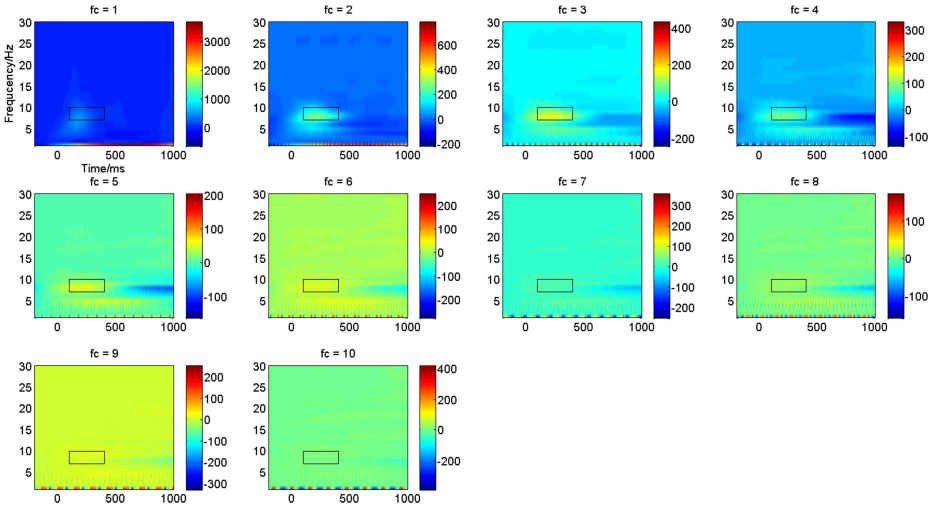

Figure 2 TFR results with CMCWT method at Cz electrode. $\sigma = 1$, the time window of the rectangle area was from 100 to 400ms and its frequency range from 7 to 10Hz.

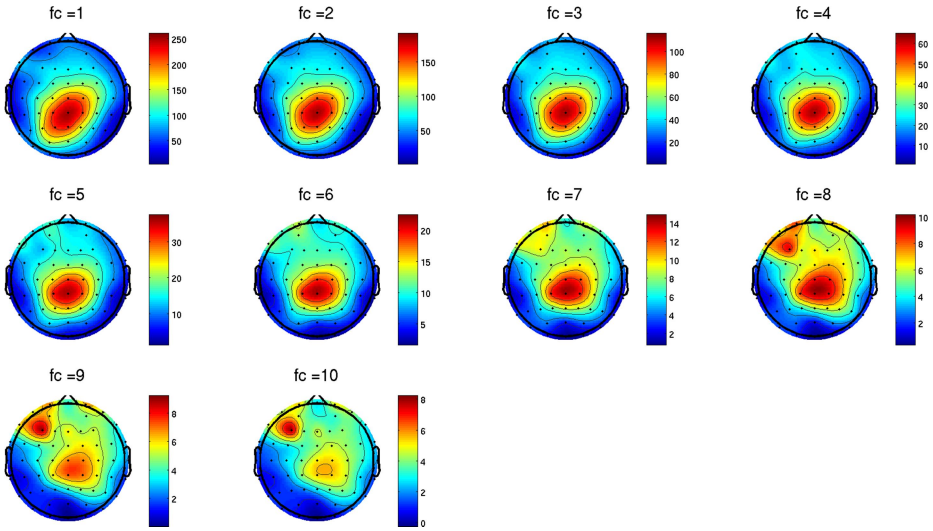

Figure 3 The corresponding topographical distribution of rectangle areas in Figure 2

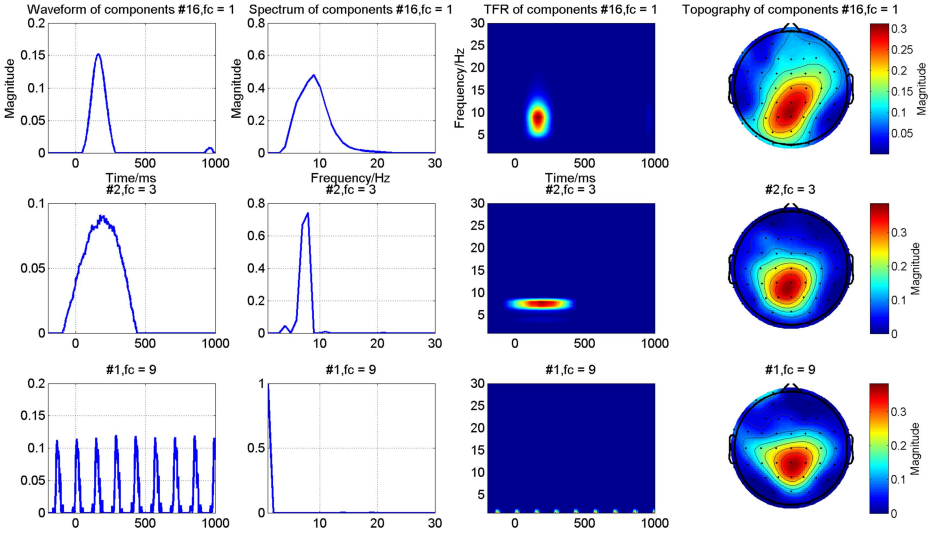

Figure 4 The corresponding temporal, spectral, and spatial components of different parameters.The third-order ERP tensor of the TFR for NCPD includes frequency (30 frequency bins), time (600 samples), and feature modes (58 channels). 21 components were extracted from each mode for NCPD, the order and variance of each component for NCPD are not determined. The TFR is based on the outer product of the temporal and spectral components.

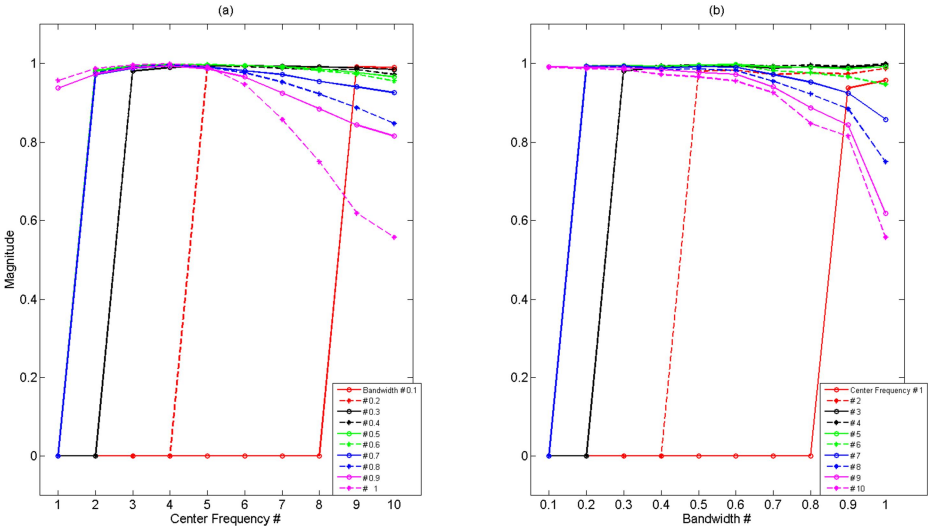

Figure 5 The Correlation coefficients between topographical distributions of each parameter and the template ($\sigma = 1, fc = 4$)

In Figure 6, the power of the region of interest (time: 100-400ms, frequency: 7-10Hz) of Cz with different parametric settings of *fc* and σ is analyzed. The first/second/third row respectively shows the *p* value of the waiting time condition/feedback condition/interaction. The figure shows how the *p* value changes with *fc*

(or σ), when σ (or fc) is a constant. When σ (or fc) is fixed, the p value shows an increasing tendency with the increasement of fc (or σ).The corresponding statistical analysis results may also differ with different settings of fc and σ.

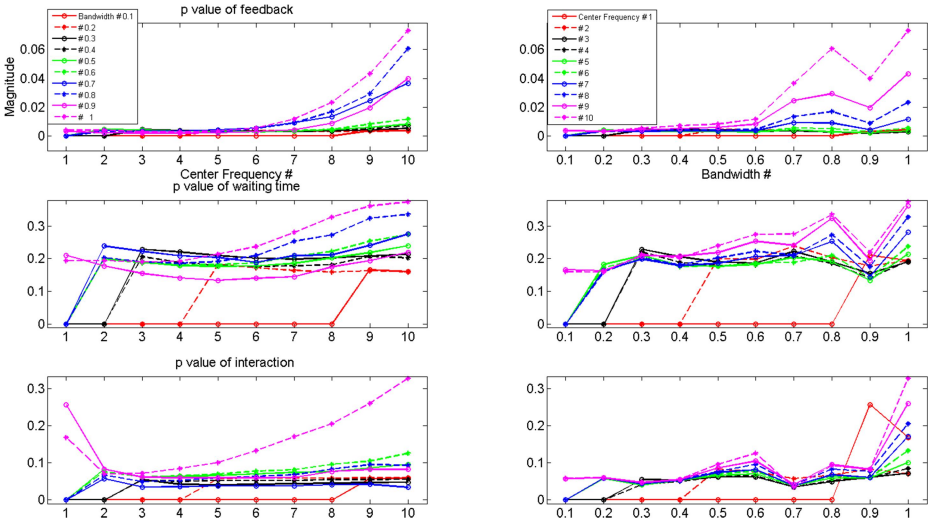

Figure 6 Two-way repeated measurements ANOVA results of different fc and σ parameters. Two factors refer to waiting time (short, long) and feedback valence (loss, gain)

5 Conclusion

The current study, through employing the methods of CMCWT, explored the influence of fc and σ variation on the time-frequency and topographical results of ERP data. Besides, NCPD was used to further confirm the differences manifested in time-frequency results. Results showed that parametric variation of σ and fc had an effect on time-frequency results. Moreover, it was found that different components would be obtained from different TFR results by NCPD. The current study therefore suggests that different parameters should be examined in order to get optimal time-frequency results. Meanwhile, the NCPD method is highly encouraged to be applied for the further confirmation of differences in time-frequency results.

6 Acknowledgments

This work was supported by National Natural Science Foundation of China (Grant No. 81471742) and the Fundamental Research Funds for the Central Universities [DUT16JJ(G)03] in Dalian University of Technology in China.

7 References

1. Niedermeyer, E. and F.L. da Silva, Electroencephalography: basic principles, clinical applications, and related fields. 2005: Lippincott Williams & Wilkins.
2. Luck, S.J., An Introduction to the Event-Related Potential Technique. 2005. 66.
3. Cong, F., et al., Linking brain responses to naturalistic music through analysis of ongoing EEG and stimulus features. IEEE Transactions on Multimedia, 2013. 15(5): p. 1060-1069.
4. Herrmann, C.S., et al., Time–frequency analysis of event-related potentials: a brief tutorial. Brain topography, 2014. 27(4): p. 438-450.
5. Sánchezǹacher, N., et al., Event-related brain responses as correlates of changes in predictive and affective values of conditioned stimuli. Brain Research, 2011. 1414(1): p. 77-84.
6. Sanchezalavez, M. and C.L. Ehlers, Event-related oscillations (ERO) during an active discrimination task: Effects of lesions of the nucleus basalis magnocellularis. International Journal of Psychophysiology Official Journal of the International Organization of Psychophysiology, 2016. 103: p. 53.
7. Mathes, B., et al., Maturation of the P3 and concurrent oscillatory processes during adolescence. Clinical Neurophysiology Official Journal of the International Federation of Clinical Neurophysiology, 2016. 127(7): p. 2599.
8. Ergen, M., et al., Time-frequency analysis of the event-related potentials associated with the Stroop test. International Journal of Psychophysiology Official Journal of the International Organization of Psychophysiology, 2014. 94(3): p. 463-72.
9. Tallon-Baudry, C., et al., Stimulus specificity of phase-locked and non-phase-locked 40 Hz visual responses in human. The Journal of Neuroscience, 1996. 16(13): p. 4240-4249.
10. Tallon-Baudry, C., et al., Induced γ-band activity during the delay of a visual short-term memory task in humans. The Journal of neuroscience, 1998. 18(11): p. 4244-4254.
11. Tallon-Baudry, C., et al., Oscillatory γ-band (30–70 Hz) activity induced by a visual search task in humans. The Journal of neuroscience, 1997. 17(2): p. 722-734.
12. Tallon-Baudry, C. and O. Bertrand, Oscillatory gamma activity in humans and its role in object representation. Trends in cognitive sciences, 1999. 3(4): p. 151-162.
13. Wang, J., et al., P300, not feedback error-related negativity, manifests the waiting cost of receiving reward information. Neuroreport, 2014. 25(13): p. 1044-8.
14. Cong, F., et al., Multi-domain feature extraction for small event-related potentials through nonnegative multi-way array decomposition from low dense array EEG. International journal of neural systems, 2013. 23(02): p. 1350006.
15. Cong, F., et al., Tensor decomposition of EEG signals: a brief review. Journal of neuroscience methods, 2015. 248: p. 59-69.
16. Delorme, A. and S. Makeig, EEGLAB: an open source toolbox for analysis of single-trial EEG dynamics including independent component analysis. Journal of neuroscience methods, 2004. 134(1): p. 9-21.